

# Femto- to Microsecond Excited State Relaxation of 9-(4-(*N,N*-Dimethylamino)phenyl)phenanthrene and 4-(9-Phenanthryl)-3,5-*N,N*-tetramethylaniline

A. Onkelinx, G. Schweitzer, F. C. De Schryver,\* H. Miyasaka, and M. Van der Auweraer

*Department of Chemistry, Katholieke Universiteit Leuven, Celestijnenlaan 200F, BE-3001 Heverlee, Belgium*

T. Asahi, H. Masuhara, and H. Fukumura

*Department of Applied Physics, Faculty of Engineering, Osaka University, Suita, Osaka 565, Japan*

A. Yashima and K. Iwai

*Department of Chemistry, Faculty of Science, Nara Women's University, Nara 630, Japan*

*Received: January 17, 1997; In Final Form: March 11, 1997*<sup>⊗</sup>

This paper discusses how the solvent-induced rapid relaxation of the initial delocalized excited state of 9-(4-*N,N*-dimethylaminophenyl)phenanthrene (9DPhen), obtained immediately after picosecond pulsed excitation, can be resolved by means of femtosecond transient absorption experiments. The results obtained for 9DPhen are compared to the results of a sterically hindered compound 4-(9-phenanthryl)-3,5-*N,N*-tetramethylaniline (3,5Me9DPhen) in order to get more information about the possible conformational relaxation process suggested for these compounds. From the results of the femtosecond transient absorption experiments, a possible model is proposed to characterize the kinetic behavior of these molecules. After photoexcitation of 9DPhen and 3,5Me9DPhen, the distribution of higher excited states shows a fast transition within a femtosecond timescale to a "hot" charge transfer state. This state loses excess energy by a relaxation process (electronic and/or vibrationally and/or conformationally relaxation) on picosecond timescale. From this relaxed excited charge transfer state, fluorescence and intersystem crossing to a triplet state originate simultaneously and in competition. From the comparison of the steady state absorption spectrum of 9DPhen and 3,5Me9DPhen, as well as the transient absorption spectra of the triplet state, one can distinguish the quite different nature of the ground and the triplet state in both compounds. The bathochromic shift of the emission spectrum of both compounds suggests a larger excited-state dipole moment for 3,5Me9DPhen compared to 9DPhen. The lower values of the radiative rate constant  $\langle k_f \rangle$  and the longer decay times of 3,5Me9DPhen correlate with a less allowed radiative transition compared to that of 9DPhen. It is suggested that for 3,5Me9DPhen, the emissive state mixes to a smaller extent with a state with a strongly allowed transition and/or that the average angle between the phenyl and phenanthrene moieties of the excited state is larger (farther away from 0) than in the unsubstituted molecule, leading to a less allowed transition and a smaller value of the rate constant of fluorescence.

## Introduction

Conformational folding bringing donor and acceptor  $\pi$ -electron systems into parallel planes, within a distance allowing through-space interactions and Coulomb stabilization of the charge-transfer (CT) state,<sup>1–6</sup> is excluded for molecules consisting of an electron donor and an electron acceptor directly connected by a single  $\sigma$ -bond. It has been shown<sup>7–30</sup> that primary excited singlet states of *p*-(9-anthryl)-*N,N*-dimethylaniline (ADMA) and related compounds undergo solvent-assisted femto- or picosecond relaxation to a polar fluorescent CT state. The geometry and electronic structure of the emitting CT state, however, are still points of discussion.<sup>5,6,11,23</sup> Okada and co-workers<sup>7–9</sup> originally explained their results in terms of an abrupt structural change of the excited ADMA when the solvent was changed from diethylether to more polar solvents.

More recent picosecond transient absorption studies by the same authors, however, show a difference between the electronic structure of the excited state of ADMA or structurally similar molecules and that of molecules with strongly orthogonal  $\pi$ -systems of the donor and the acceptor (e.g., 4-(9-anthryl)-

*N,N*-2,6-tetramethylaniline).<sup>23,26,32</sup> They showed that the transient absorption spectra of ADMA in medium polar solvents cannot be presented by a linear combination of the anthracene-like band in weakly polar solvents and the anthracene anion radical band in strongly polar solvents. They therefore expressed doubts as to the validity of the simple two-state TICT (twisted intramolecular charge transfer) model for ADMA and related compounds<sup>11,31</sup> according to which the excited singlet state undergoes an adiabatic intramolecular electron transfer and where two metastable states are assumed to interconvert by a torsion motion, which provides a possible reaction coordinate for the electron transfer. It seems to be necessary to invoke "multiple states" with different degrees of charge transfer and twisting angle, depending on the interaction with solvent.

A similar conclusion was also reached in recent quantum chemical calculations,<sup>33</sup> where twist angle dependent values of transition energies, oscillator strengths, and dipole moments were calculated. Also, here the authors expressed doubts as to the validity of the simple two-state TICT model. Recently,<sup>34</sup> a CT absorption band in the spectrum of 9-(4-*N,N*-dimethylaminophenyl)phenanthrene (9DPhen; Figure 1) has been detected, which indicates an interaction between the dimethylanilino- and the phenanthrene subunits in the ground state.

\* To whom correspondence should be addressed.

<sup>⊗</sup> Abstract published in *Advance ACS Abstracts*, June 15, 1997.

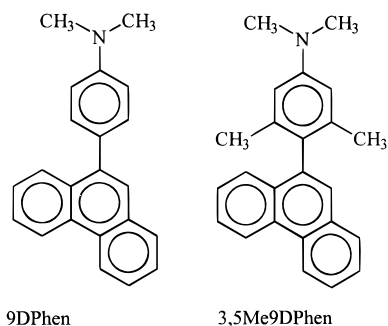


Figure 1. Structures of 9DPhen and 3,5Me9DPhen.

The dipole moment value and the resulting bathochromic shift of the emission spectrum in polar solvents give clear evidence that the emitting excited state in highly polar solvents has a pronounced charge-transfer character. The quantum yield of fluorescence ( $\Phi_f$ ) of 9DPhen is high and increases with increasing solvent polarity. The formation of this intramolecular charge-transfer (ICT) state in excited 9DPhen has been discussed previously<sup>34</sup> in terms of a model involving either mixing of states and/or configurations, as influenced by geometrical changes and solvent polarity. According to this model, the fluorescence rate constant  $k_f$  is first increasing upon increasing solvent polarity because of the narrowing of the energy difference of ICT and  $S_1$  or  $S_2$  states and then decreasing again in highly polar solvents.

To get more insight into the nature of the fluorescent state(s) and/or conformers of this class of compounds, a sterically hindered molecule has been synthesized, namely, 4-(9-phenanthryl)-3,5-*N,N*-tetramethylaniline (3,5Me9DPhen; Figure 1). Owing to the steric hindrance, the phenanthryl subunit is twisted more out of the phenyl plane, leading to a possible decoupling of the phenanthrene and dimethylanilino subunits. In this contribution, the solvent dependence of the spectral position of the CT fluorescence maximum ( $\bar{\nu}_{\max}^{\text{ct}}$ ), the quantum yield of fluorescence ( $\Phi_f$ ), and the excited state relaxation kinetics ( $\langle\tau_f\rangle$ ) of 3,5Me9DPhen are discussed and compared to the respective data of 9DPhen.

To get a better insight into the excited state kinetics, single photon timing (SPT) experiments are combined with femtosecond transient absorption spectroscopy in an apolar and a polar solvent. For analogous compounds, it has been suggested that the primary excited singlet state undergoes a solvent assisted femto- or picosecond relaxation to a polar fluorescent CT state.<sup>7–30</sup> Nanosecond transient absorption measurements were performed to obtain more information about the nature of the triplet state and, more important, to characterize the quite different triplet states of 9DPhen and 3,5Me9DPhen.

For 3,5Me9DPhen it was possible to separate the rate constant of internal conversion  $k_{\text{ic}}$  and the rate constant of intersystem crossing  $k_{\text{isc}}$  from the rate constant of nonradiative decay  $k_{\text{nr}}$  by means of laser-induced optoacoustic spectroscopy (LIOAS) experiments in apolar and polar solvents.

## Experimental Section

**Synthesis.** The synthesis of 9-(4-*N,N*-dimethylaminophenyl)-phenanthrene (9DPhen) has been described earlier.<sup>34</sup> 4-(9-Phenanthryl)-3,5-*N,N*-tetramethylaniline (3,5Me9DPhen) was synthesized by the Grignard coupling reaction<sup>35</sup> of the Grignard reagent prepared from 4-bromo-3,5-*N,N*-tetramethylaniline<sup>36</sup> with 9-bromophenanthrene using dichloro[1,3bis(diphenylphosphino)propane]nickel(II) as catalyst in dry THF, similar to the 9-(4-*N,N*-dimethylamino)phenyl)phenanthrene<sup>34</sup> synthesis. The crude product was purified by column chromatography on silica gel with benzene eluent and recrystallized from toluene,

mp 183.1–184.6 °C. EIMS(70 eV):  $m/e$  (relative intensity) 325( $M^+$ ,100), 324(18), 265(11), and 162.5( $M^{2+}$ ,11). <sup>1</sup>H NMR ( $\text{CDCl}_3$ ):  $\delta$  1.95 (6H,s), 3.04 (6H,s), 6.60 (2H,s), 7.42–8.80 (9H,m).

All products used for stationary and time-resolved fluorescence experiments as well as femtosecond transient absorption experiments were further purified using HPLC with 1:9 v/v ethyl acetate with hexane as the eluent.

**Solvents.** All solvents used (isooctane, hexane, diethyl ether, ethyl acetate, and acetonitrile (ACN)) were of spectroscopic grade and used as received.

**Experimental Methods.** Steady-state absorption spectra were recorded on a Perkin Elmer Lambda 6 UV-vis spectrophotometer. Corrected fluorescence spectra were obtained with a SPEX Fluorolog 212. The fluorescence quantum yields were determined using quinesulphate in 0.1 N  $\text{H}_2\text{SO}_4$  ( $\Phi_f = 0.54$ ) as a reference.<sup>37</sup> The absorption of the sample solutions used for the stationary and time-resolved fluorescence experiments equals  $0.1 \text{ cm}^{-1}$  at the excitation wavelength ( $\lambda_{\text{excitation}} = 295 \text{ nm}$ ).

Stationary and time-resolved fluorescence measurements were performed on samples degassed by several freeze–pump–thaw cycles.

Time-resolved fluorescence decays were obtained by the single photon timing (SPT) technique, and the fluorescence decays were analyzed by global analysis, using the reference convolution method.<sup>38–40</sup>

For the SPT experiments the excitation wavelength was 295 nm (prompt response of scatter solution is 40 ps fwhm) and the decays were measured over the whole emission range. For 9DPhen, the measured ranges for various solvents are the following: isooctane, 370–470 nm; diethyl ether 380–460 nm; ethyl acetate, 390–540 nm; acetonitrile, 380–530 nm. For 3,5Me9DPhen, the ranges are the following: isooctane, 350–400 nm; diethylether, 380–480 nm; ethylacetate, 420–500 nm; ACN, 450–550 nm. All fluorescence decays were recorded at the magic angle ( $55^\circ$ ) configuration, contained  $10^4$  peak counts, and were collected in 511 channels of the multichannel analyzer. Time increments of 236, 40, 87, and 174 ps were used for 3,5Me9DPhen in isooctane, diethyl ether, ethyl acetate, and acetonitrile, respectively, and 60 and 81 ps for 9DPhen in isooctane and acetonitrile.

POPOP (*p*-bis[2-(5-phenyloxazolyl)]benzene) in methylcyclohexane and PPO (2,5-diphenyloxazole) in methylcyclohexane, having a decay time ( $\tau_{\text{ref}}$ ) of 1.1 and 1.4 ns, respectively, were used as reference compounds. The reference samples were degassed by several freeze–pump–thaw cycles before use.

For the nanosecond transient absorption experiments, the absorption at the excitation wavelength (320 nm) is  $1.5 \text{ cm}^{-1}$ . The nanosecond laser photolysis system<sup>41</sup> has been described in detail elsewhere.

For the femtosecond transient absorption experiments, the absorption of the sample solutions equals  $15 \text{ cm}^{-1}$  at the excitation wavelength (260 nm) and a cell with an optical path length of 2 mm is used. The solutions were degassed and the cells sealed. The femtosecond transient absorption spectroscopic system is similar to that reported previously.<sup>42</sup> An excitation light source consists of a CW self-mode-locked Ti:sapphire laser (Mira 900 Basic, Coherent), pumped by an  $\text{Ar}^+$  laser (Innova 310, Coherent), and a Ti:sapphire regenerative amplifier system (TR70, Continuum) with a Q-switched Nd:YAG laser (Surelight I, Continuum). The fundamental output from the regenerative amplifier (780 nm, 3–4 mJ/pulse, 170 fs fwhm, 10 Hz) was frequency tripled (260 nm) and used as an excitation light source. Typically, its energy was less than  $1 \text{ mJ/cm}^2$ . The

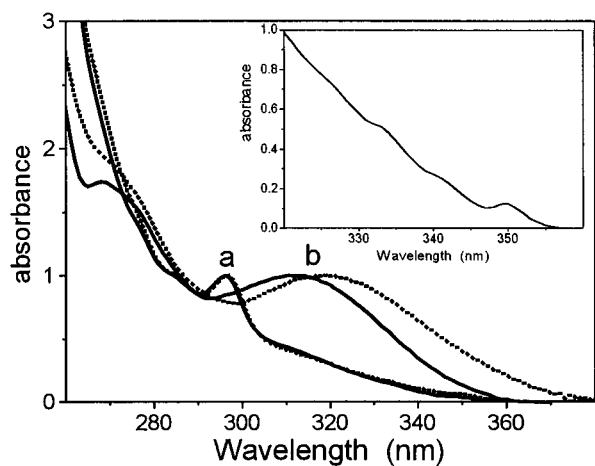


**Figure 2.** Absorption spectrum of (a) 3,5Me9DPhen and (b) 9DPhen in isooctane (—) and ACN (---) at room temperature. Insert shows an enlarged spectrum of 3,5Me9DPhen in isooctane.

residual of the fundamental output was focused into a quartz cell (1 cm path length) containing H<sub>2</sub>O to generate a white-light continuum. The continuum pulse was divided into two, one being used as a probe beam and the other as a reference beam to correct shot-to-shot variation of spectral shapes and intensity of the probe beam. The transmitted light of the probe beam through a sample was detected by a multichannel spectrometer (HH4-0913, Otsuka Electronics). The reference beam was led to another multichannel spectrometer. Typically, the spectral data were averaged over 300 measurements. The time delay between the pump and the probe pulses is regulated by an optical delay circuit with a computer-controlled stepping motor.

## Results and Discussion

**Absorption and Emission Experiments as a Function of the Solvent Polarity.** As can be seen in Figure 2, the absorption spectrum of 3,5Me9DPhen does not show the strong CT absorption band compared to 9DPhen.<sup>34</sup> The maximum of 350 nm and the shoulders at 340 and 333 nm in the absorption spectrum of 3,5Me9DPhen are quite comparable with those of the L<sub>b</sub> transition of 9-ethylphenanthrene (maximum at 349, 340, 332, 325, and 317 nm).

In contrast to the bathochromic shift of the CT absorption band of 9DPhen with increasing solvent polarity, the position of the maximum of the absorption spectrum of 3,5Me9DPhen is independent of the solvent, which is an indication of a decoupling between the phenanthrene and the dimethylanilino moiety in the ground state.

The emission spectra of 3,5Me9DPhen (Figure 3) consist of a structureless emission band in medium-polar and polar solvents at room temperature. In the apolar solvent isooctane, some fine structure is observed, but it is small compared to the fine structure in the emission spectrum of ethylphenanthrene and phenylphenanthrene.<sup>34</sup> The emission spectra of 3,5Me9DPhen show a strong bathochromic shift when the polarity of the solvent increases from isooctane to acetonitrile, indicating a substantial dipole moment in the excited state.

In Table 1, the emission maxima of 3,5Me9DPhen are listed together with the emission maxima of 9DPhen. The wavelength shift between isooctane and acetonitrile corresponds for 3,5Me9DPhen to an energy difference of 8000 cm<sup>-1</sup>, again indicating a polar emissive state. The fluorescence quantum yields of 9DPhen and 3,5Me9DPhen are reported in Table 1 together with those of 9DPhen. Similar to 9DPhen, the quantum

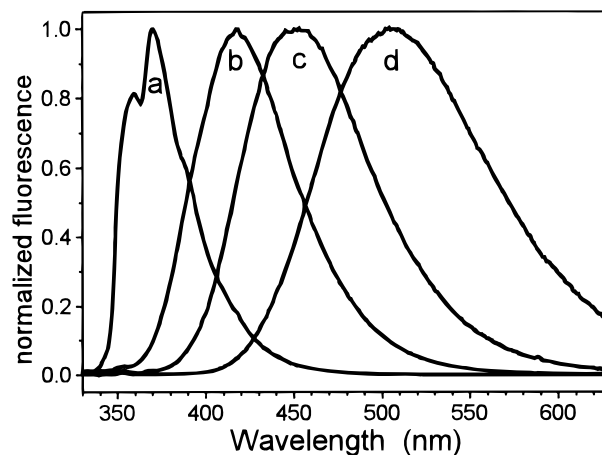


**Figure 3.** Emission spectrum of 3,5Me9DPhen in solvents of different polarity: (a) isooctane; (b) diethyl ether; (c) ethyl acetate; (d) acetonitrile. The excitation wavelength is 320 nm.

yields of 3,5Me9DPhen are increasing with increasing solvent polarity, but in the polar solvent ACN the quantum yield is decreasing again. Generally, the value of the quantum yield of fluorescence of 9DPhen is substantially higher than the one of 3,5Me9DPhen.

**Single Photon Timing Experiments.** The results from the SPT experiments are presented in Table 1. By single decay analysis as well as by global analysis, the fluorescence decays of 3,5Me9DPhen in isooctane, diethyl ether, ethyl acetate, and acetonitrile could be fitted by a single exponential decay with the resulting decay time independent of the analysis wavelength over the whole spectral range measured. In all solvents, the decay times of 3,5Me9DPhen are increased by a factor of 2 compared to those of 9DPhen. If the calculated values of the quantum yields of fluorescence are combined with the decay time values resulting from the single photon timing experiments, the rate constant of fluorescence can be obtained,  $\langle k_f \rangle_\theta = \Phi_f / \langle \tau \rangle$ , with the assumption that the emission of 3,5Me9DPhen emanates from a charge-transfer state formed more quickly than the time resolution of the experiment.

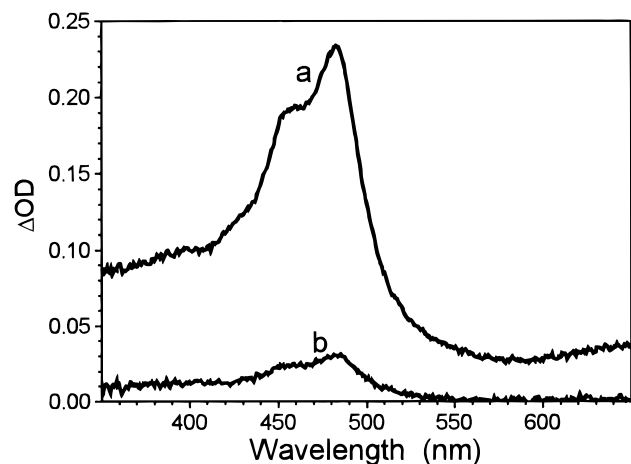
In analogy with 9DPhen,<sup>34</sup> in 3,5Me9DPhen a broadened potential minimum is assumed to be due to a rotational distribution of conformers in the emitting state, that changes with solvent polarity. This is the reason why the effective  $\langle k_f \rangle_\theta$  for 3,5Me9DPhen can be written more accurately as an average value over the different dihedral angles ( $\theta$ ) between the dimethylaniline and phenanthrene unit. The lower values of the radiative rate constant  $\langle k_f \rangle_\theta$  and the longer decay times of 3,5Me9DPhen correlate with a less allowed radiative transition compared to that of 9DPhen. This suggests that for 3,5Me9DPhen, the emissive state mixes to a smaller extent with a state with a strongly allowed transition and/or the average angle between the phenyl and phenanthrene moieties of the excited state is larger (farther away from 0) than in the unsubstituted molecule, leading to a less allowed transition and a smaller value of the rate constant of fluorescence.

**Microsecond Transient Absorption Experiments.** When the microsecond transient absorption spectra of 3,5Me9DPhen in solvents of different polarity were measured (Figure 4), a different absorption spectrum was obtained compared to that of 9DPhen. In the latter a broad absorption was observed between 350 and 750 nm, the maximum of which was changing as a function of the solvent polarity.<sup>34</sup>

In 3,5Me9DPhen, however, a narrow absorption band was observed in the apolar and medium-polar solvents with two maxima at 460 and 480 nm, respectively. Because of its

**TABLE 1: Solvent Effects on the Spectral Position of the CT Fluorescence Maxima, Quantum Yields for Fluorescence, and Decay Parameters of (A) 9DPhen and (B) 3,5Me9DPhen**

	$\tilde{\nu}_{\max}$ (cm <sup>-1</sup> )		$\Phi_f$		$\tau$ (ns)		$k_f$ (10 <sup>7</sup> s <sup>-1</sup> )		$\tilde{\nu}^3$ (10 <sup>-7</sup> s <sup>-1</sup> cm <sup>3</sup> )	
	A	B	A	B	A	B	A	B	A	B
isooctane	25939	27777	0.36	0.16	9.2	21.3	3.9	0.75	8	1.29
diethyl ether	24570	23923	0.49	0.21	2.2	3.8	22.7	5.53	62	16.3
ethyl acetate	23255	22173	0.65	0.27	3.6	8.5	18.1	3.1	56	11.01
ACN	21321	19724	0.85	0.22	7	19.1	12	1.15	51	6.14

**Figure 4.** Triplet transient absorption spectrum of 3,5Me9DPhen in diethyl ether at different delay times: (a) 100 ns; (b) 10  $\mu$ s. The excitation wavelength is 320 nm.

similarity to the  $T_1$ - $T_n$  absorption of phenanthrene,<sup>43</sup> we attribute this to a triplet state. Because of the analogy between the absorption spectrum of phenanthrene and 3,5Me9DPhen, a local triplet is assumed in this case, in contrast to the delocalized triplet in 9DPhen.

In the solvent acetonitrile, the overall shape of the transient absorption band is analogous, but the relative intensity of the absorption band at 460 nm is increased slightly compared to the data from the other solvents.

**Femtosecond Transient Absorption Experiments on 9DPhen and 3,5Me9DPhen in an Apolar and a Polar Solvent.** The picosecond transient absorption experiments were described previously for 9DPhen in an apolar and a polar solvent (isooctane and acetonitrile, respectively).<sup>34</sup> In acetonitrile, a rapid decay within a few picoseconds from a less polar but delocalized excited state toward a more polar intramolecular charge transfer (ICT) state was found. In order to further investigate this fast decay, femtosecond transient absorption experiments were performed for 9DPhen and 3,5Me9DPhen, both in hexane and acetonitrile. In Figures 5–8, the results are presented for different delay times in both solvents.

*9DPhen in Hexane and Acetonitrile.* As can be seen in Figure 5, the initial transient absorption shows a broad band with a maximum at around 520 nm. However, at longer delay times, the shape of the spectrum at the blue edge is changed and an additional shoulder at shorter wavelengths (470 nm) appears.

In acetonitrile (Figure 6), a similar spectral change of the absorption did occur. However, the resulting absorption band at 480 nm is sharper than the one in hexane. The spectral position is similar to the one of the radical cation of dimethylaniline (473 nm).<sup>44</sup> However, the absorption band is not as sharp as in the case of dimethylaniline, which we attribute to the extensive coupling between the two subunits in 9DPhen.

*3,5Me9DPhen in Hexane and Acetonitrile.* For the sterically hindered compound 3,5Me9DPhen in hexane (Figure 7), the absorption band directly after excitation is almost identical to the absorption band observed for 9DPhen in the same solvent.

However, all the spectral changes occurring in the absorption spectrum for this system seem to be completed in a shorter time. Moreover, the shape of the absorption spectrum in the wavelength region of 480 nm of 3,5Me9DPhen at longer delay times is sharper compared to the transient absorption spectrum of 9DPhen, suggesting a narrower distribution of the intramolecular twist angle with an average closer to 90°.

In acetonitrile (see Figure 8), the position and the spectral shape of the initial absorption band are quite comparable to the results obtained in hexane. However, within a very short time the excited state is changed from a “delocalized state” to a radical cation state. In this solvent, the absorption spectrum of the cation is very sharp and very similar to the one of the free radical cation of dimethylaniline. One has to keep in mind, however, that since the absorption spectra mentioned above do not represent species-associated spectra, they do not allow for direct extraction of kinetic data.

*Data Analysis.* To analyze the data for each compound, the originally recorded set of spectra was converted into a set of decay curves at eight fixed wavelengths. The data handling included a correction for the wavelength dispersion of the white-light continuum. After correction, in a nonlinear least-squares fit procedure, a function consisting of a sum of four exponentials was fitted to the data sets.

$$a(t)_\lambda = \sum_{i=0}^3 \alpha_i \exp(-t/\tau_i) \quad (1)$$

In all data sets, a very long  $\tau_0$  ( $\mu$ s) with amplitude  $a_0$  was found, which we attributed to the relaxation of the triplet state and treated as a constant.

The long-lived nonconstant component 3 can be attributed to the fluorescence decay. Since this is known from previous SPT measurements,  $\tau_3$  was fixed to this value during all fits. However,  $\alpha_3$  was not held constant. As a next step, in a short time analysis window (10 ps)  $\alpha_1$  and  $\tau_1$  were determined separately. A typical example is shown in Figure 9. Over all decays, a constant value for  $\tau_1$  with a varying  $\alpha_1$  was found. The value of  $\tau_1$  was used in the next analysis step, where  $\tau_2$  and  $\alpha_2$  were determined using a larger (500 ps) time window. When  $\tau_1$  and  $\tau_3$  are kept constant at the determined values,  $\tau_2$  is calculated by minimizing the global  $\chi^2$  values. The results of the analysis for both compounds and solvents are summarized in Table 2, and the corresponding decay-associated spectra (DAS) are shown in Figure 10.

In order to interpret the results of this data analysis, we assumed a model that includes a very fast irreversible depopulation of the Franck–Condon excited state.<sup>45</sup> Only in this case (i.e., assuming no back reaction) is it possible to assign the amplitudes ( $\alpha_1$ ,  $\alpha_2$ , and  $\alpha_3$ ) to the respective excited states directly (vide infra).

The finding of two components with a time constant less or equal than 20 ps is consistent with the results from SPT measurements performed earlier, yielding a single exponential decay with a decay time of several nanoseconds (vide infra), since the temporal resolution in those experiments was technically limited to about 20 ps.

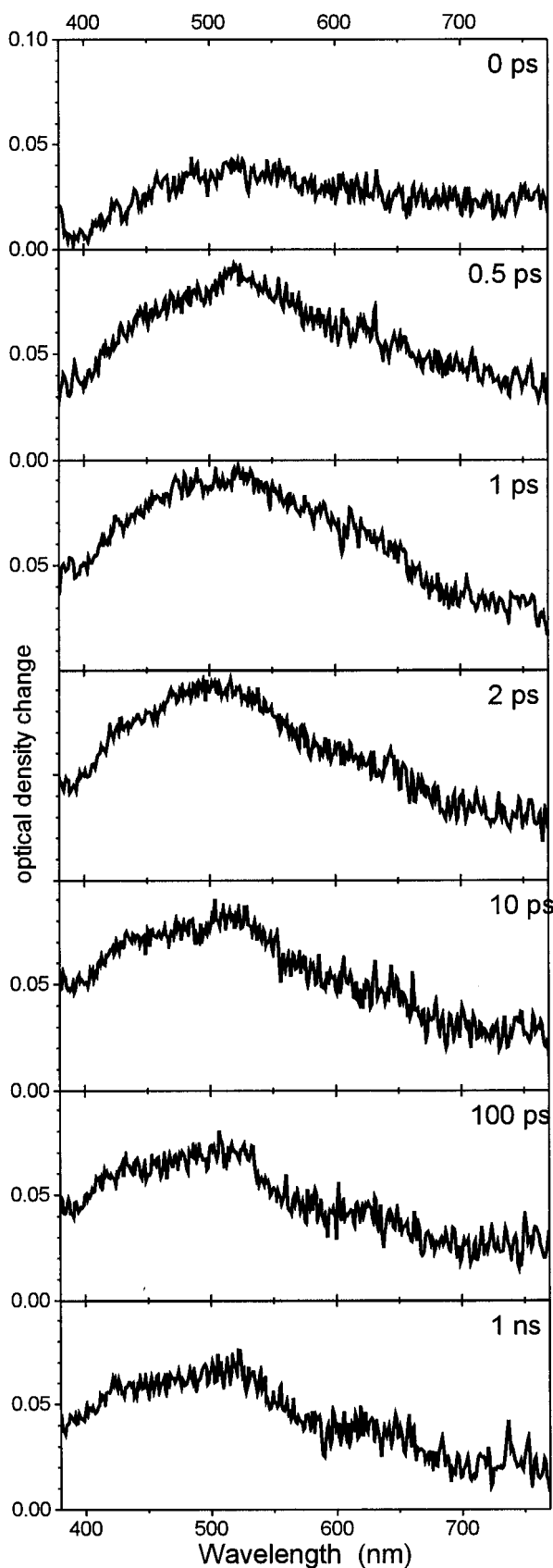


**Figure 5.** Femtosecond transient absorption spectra of 9DPhen in hexane at different delay times.

*Results and Discussion.* For 9DPhen in hexane, the  $\alpha_1$  value in the three-exponential fit of the decays is negative at all wavelengths investigated. The resulting time constant  $\tau_1$  is approximately 500 fs (i.e., slightly longer than the width of the exciting pulse). This observation implies that the energy level

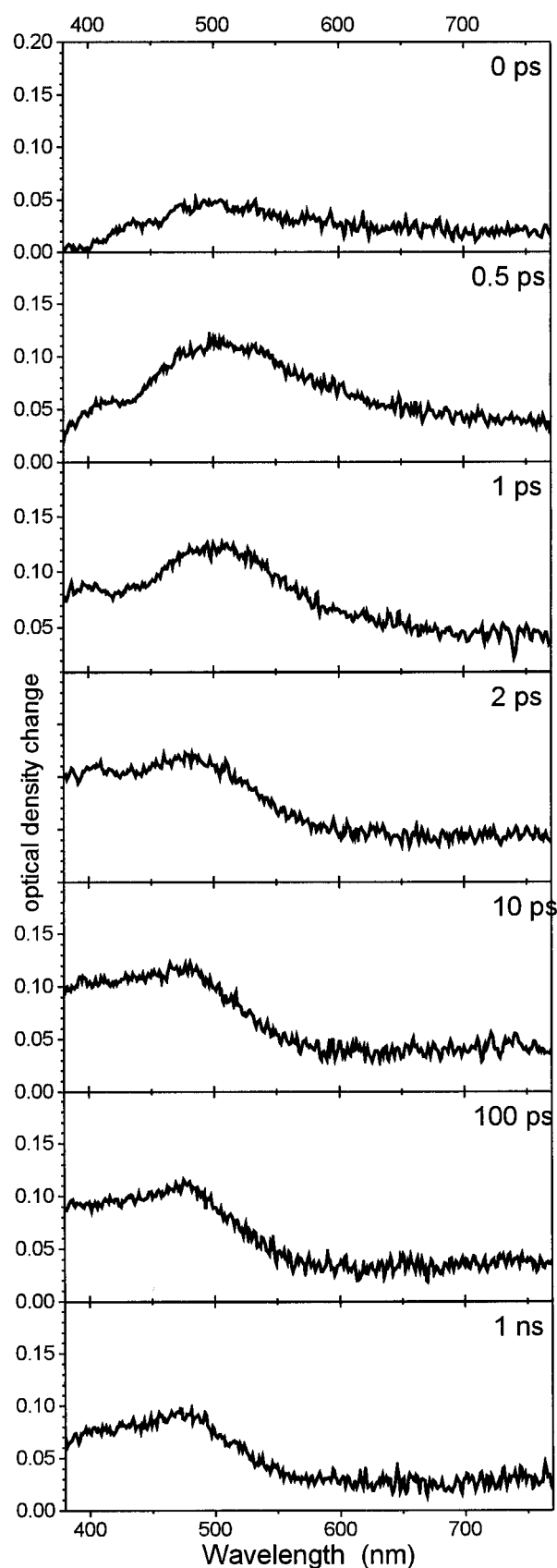


**Figure 6.** Femtosecond transient absorption spectra of 9DPhen in acetonitrile at different delay times.

where the transient absorption starts is not formed directly upon excitation but via an initially excited state that cannot be observed in our experiments directly. In the present case, this means that within the width of the laser pulse a new excited state is formed from the initially excited state.

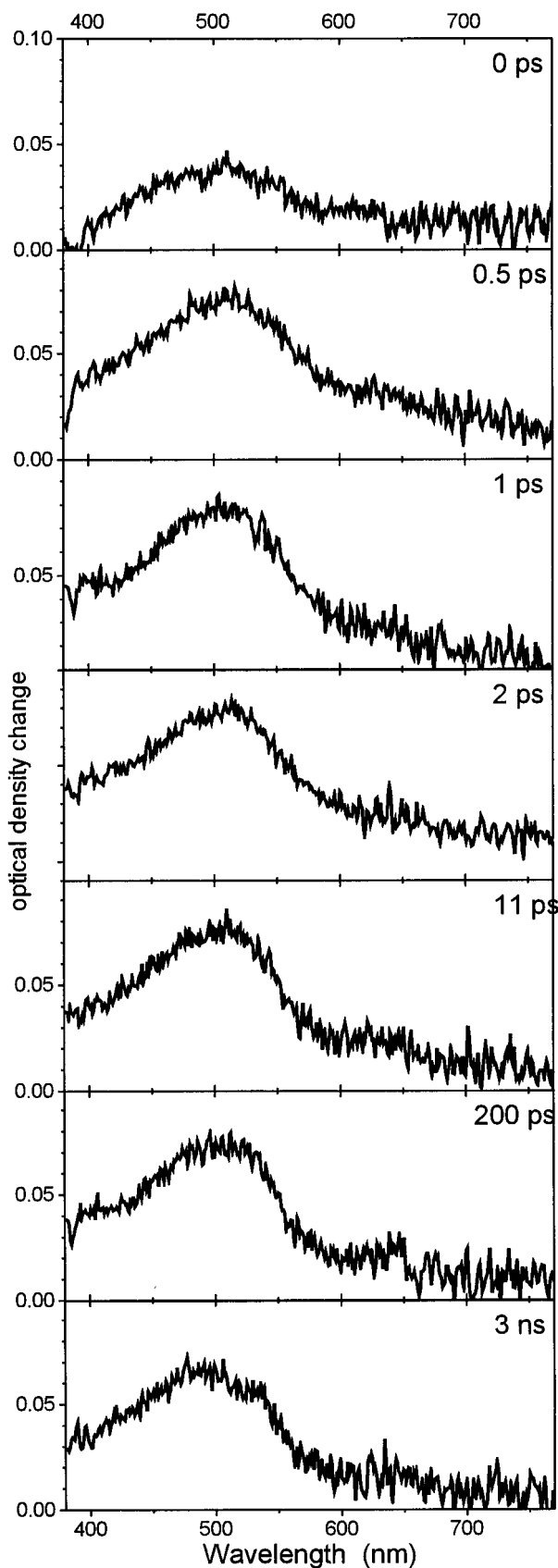


**Figure 7.** Femtosecond transient absorption spectra of 3,5Me9DPhen in hexane at different delay times.

The  $\alpha_3$  value for 9DPhen in hexane is positive at wavelengths lower than 515 nm and negative at longer wavelengths. This change of the sign of  $\alpha_3$  can be explained by a model in which two competing processes originate from the relaxed excited state: fluorescence and intersystem crossing. The latter popu-

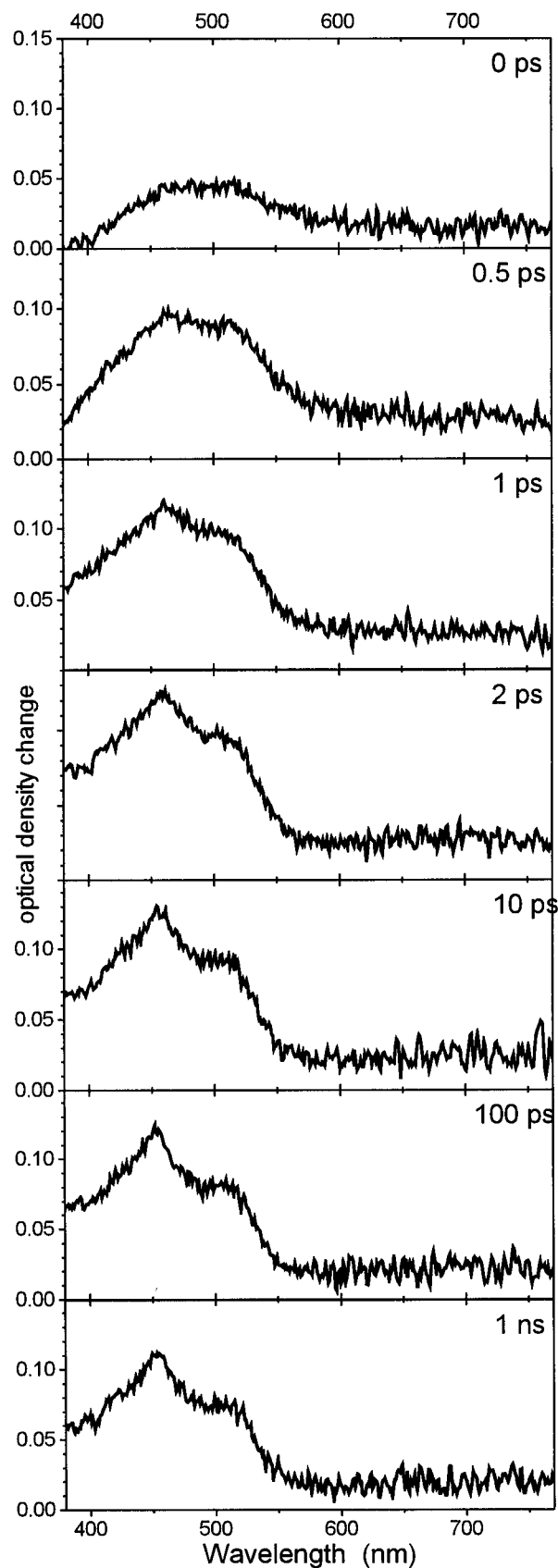


**Figure 8.** Femtosecond transient absorption spectra of 3,5Me9DPhen in acetonitrile at different delay times.

lates a triplet state that absorbs at wavelengths longer than 500 nm. This assignment is consistent with the results from the earlier nanosecond transient absorption measurements<sup>34</sup> where a  $T_1-T_n$  absorption is found in the wavelength region around 580 nm. The tendency to a negative value of  $\alpha_3$  in the

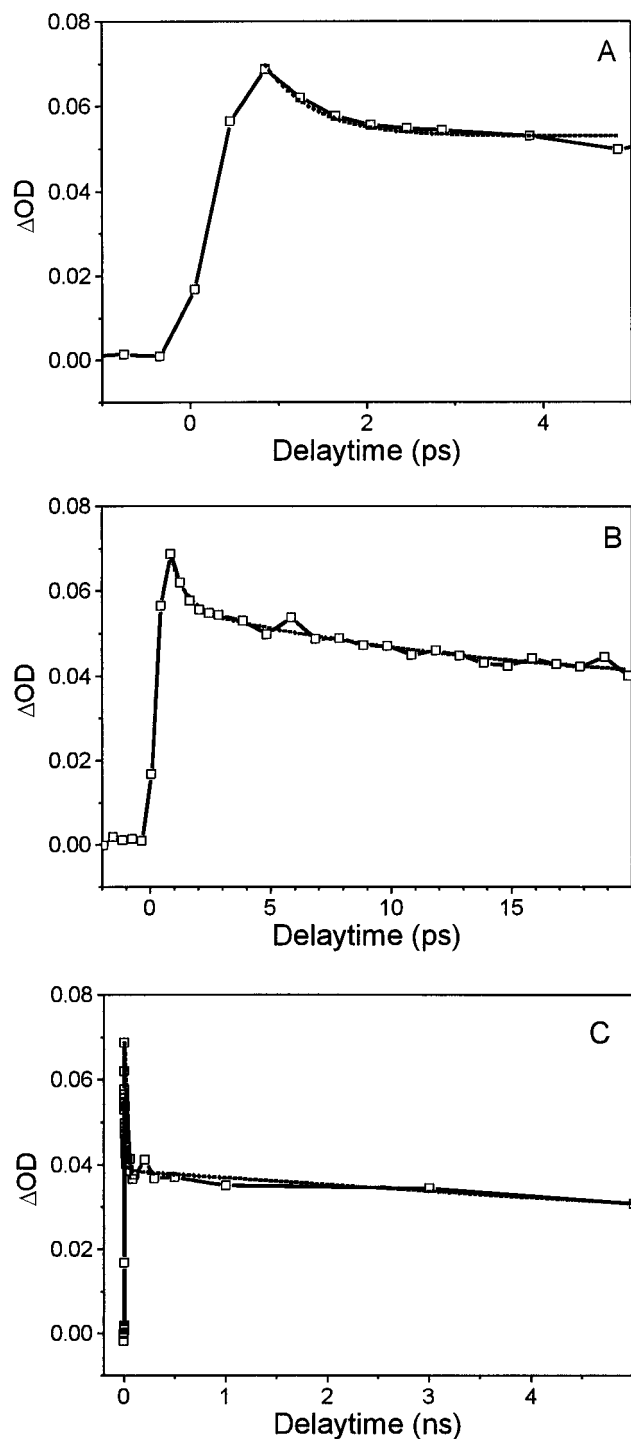


**Figure 9.** Example of an exponential fit in the (A) short time window (0–5 ps), (B) the intermediate time window (0–20 ps), and (C) the long time window (0–5000 ps).

**TABLE 2:  $\tau$  Values for (A) 9DPhen and (B) 3,5Me9DPhen**

	A $\tau_1$ (fs)	B $\tau_1$ (fs)	A $\tau_2$ (ps)	B $\tau_2$ (ps)	A $\tau_3$ (ns)	B $\tau_3$ (ns)
hexane	~500	~500	12–19	11–22	9	21
acetonitrile	700	570	16–26	8–15	7	19

wavelength region below 400 nm can be explained by a ground-state recovery process, since in this wavelength region a stationary absorption is observed.<sup>34</sup>

As can be seen in Figure 10a,  $\alpha_2$  has a positive sign over the whole absorption range and a corresponding decay time of about 15 ps. We tentatively assign this component to a relaxation from a vibrationally excited charge-transfer state (formed within

the width of the laser pulse, vide supra) to a relaxed excited charge-transfer state from which the fluorescence occurs. The finding that  $\alpha_2$  has a small value over the whole emission range could be explained by the large spectral overlap between the relaxed and the “hot” charge-transfer state.<sup>46</sup>

The overall shape of the  $\alpha_1$  value of 9DPhen in acetonitrile (Figure 10b) is similar to that in hexane, but a slightly longer time constant of 700 fs is observed. One important difference, however, is that  $\alpha_1$  takes positive values in acetonitrile for wavelengths longer than 490 nm, whereas it is negative for all measured wavelengths in hexane. We thus assume that all spectral properties in acetonitrile, including the wavelength at which  $\alpha_1$  becomes zero, are blue-shifted compared to hexane. This is consistent with results from nanosecond transient absorption spectroscopy giving a similar shift for the  $S_1$ – $S_n$  transition.<sup>34</sup>

The value of  $\alpha_3$  ( $\tau_3 = 7$  ns) is positive over the absorption range studied, but there is a clear tendency to negative  $\alpha_3$  values for wavelengths longer than 550 nm. Such a crossover at longer wavelengths is again consistent with the nanosecond transient absorption measurements (vide supra), since the  $T_1$ – $T_n$  absorption band yielding a negative  $\alpha_3$  value is shifted to longer wavelengths when the solvent polarity is increased.<sup>34</sup>

The most pronounced difference between 9DPhen and 3,5Me9DPhen is found in the shape of amplitude  $\alpha_3$  (see Figure 10d), which in the case of 3,5Me9DPhen has positive values over the whole wavelength range investigated here. This finding is very important and is again consistent with the results from nanosecond transient absorption experiments, where in contrast to 9DPhen, no  $T_1$ – $T_n$  absorption in the region of 560–580 nm was found for this compound. This overall consistency, in turn, is yielding additional support for our assignment of component 3 as stated above.

If the model compound 9PhPhen in hexane is analyzed according to the same procedure, two decay constants can be distinguished ( $\tau_1 = 500$  fs and  $\tau_2 = 41$  ns).

**Laser-Induced Optoacoustic Spectroscopy (LIOAS) Experiments in Solvents of Different Polarity.** To separate the contribution of  $k_{isc}$  and  $k_{ic}$  from the nonradiative rate constant  $k_{nr}$  of 3,5Me9DPhen, optoacoustic experiments were conducted using LIOAS in solvents of different polarity.

In Figure 11, the Jablonski diagram is presented, which was proposed by the femtosecond transient absorption experiments and used to calculate the values of  $\alpha$  and  $\beta$ .

$$\alpha = E_{th}/E_{abs} \quad (2)$$

$$\beta = \frac{k_{ic}}{k_{isc} + k_{ic}} \quad (3)$$

$$\alpha h\nu_{excit} = E(S_1^* - CT) + \Phi_f E(S_0^* - S_0) + \Phi_{ic} E(S_1 - S_0) + \Phi_{isc} E(S_1 - T_1) \quad (4)$$

where  $(S_1^* - CT)$  corresponds to the energy difference between the excitation energy ( $31\,250\text{ cm}^{-1}$ ) and the onset of the emission ( $\text{cm}^{-1}$ ),  $(S_0^* - S_0)$  is the energy difference between the onset of the emission and the maximum of the emission ( $\text{cm}^{-1}$ ),  $(S_1 - S_0)$  equals the onset of the emission ( $\text{cm}^{-1}$ ), and  $(S_1 - T_1)$  corresponds to the energy difference between the onset of the emission and the onset of the phosphorescence ( $21\,367\text{ cm}^{-1}$ ). For all solvents used, the results of the calculated rates of intersystem crossing and internal conversion of 3,5Me9DPhen are presented in Table 3, along with the energy differences used in eq 4, for the solvents used.

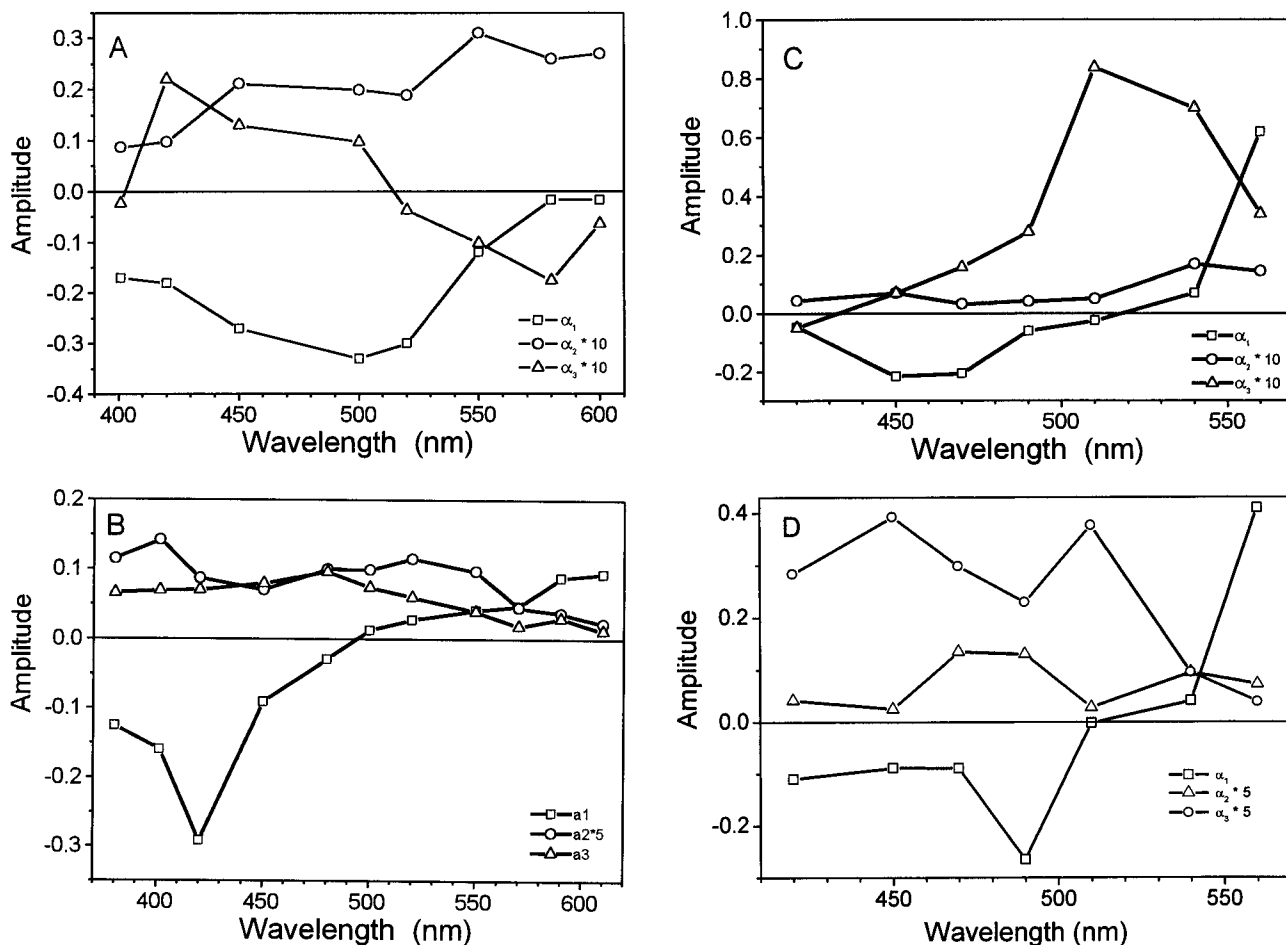


**Figure 10.** Progress of the amplitudes of the obtained three-exponential function as a function of the emission wavelength (nm) for 9DPhen in (A) hexane and in (B) acetonitrile and for 3,5Me9DPhen in (C) hexane and in (D) acetonitrile.

**TABLE 3: Rates of Intersystem Crossing and Internal Conversion of 3,5Me9DPhen and Energy Differences**

	$k_{nr}$ ( $10^7 \text{ s}^{-1}$ )	$\alpha$	$\beta$	$k_{ic}$ ( $10^7 \text{ s}^{-1}$ )	$k_{isc}$ ( $10^7 \text{ s}^{-1}$ )	( $S_1^* - CT$ ) ( $\text{cm}^{-1}$ )	( $S_0^* - S_0$ ) ( $\text{cm}^{-1}$ )	( $CT - S_0$ ) ( $\text{cm}^{-1}$ )	( $CT - T_1$ ) ( $\text{cm}^{-1}$ )
isooctane	3.94	0.21	$\sim 0$	0	3.94	1577	2646	29673	8306
diethyl ether	20.8	0.33	0.063	1.3	19.5	3395	3932	27855	6488
ethyl acetate	8.38	0.29	0.21	1.75	6.62	4795	4283	26455	5088
ACN	4.08	0.33	$\sim 0$	0	4.08	6125	5402	25125	3758

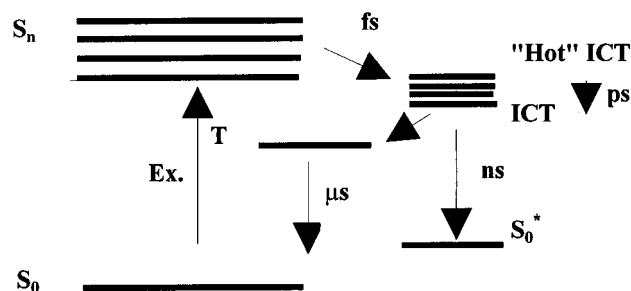


**Figure 11.** Jablonski diagram used to calculate  $\alpha$  and  $\beta$ .

As can be seen from Table 3, for apolar and polar solvents, the nonradiative rate constant  $k_{nr}$  is completely due to intersystem crossing to the triplet state whereas in medium-polar solvents internal conversion is getting more important. As described earlier (vide infra), the triplet state of 3,5Me9DPhen has the same nature as the localized triplet state in 9-ethylphenanthrene. Because of this reason one can assume that the molar volume in the ground and excited state is the same and that the measured optoacoustic signal is only due to the

contraction or expansion of the medium caused by the release of heat.

For 9DPhen, however, an analysis of  $k_{nr}$  by means of optoacoustic experiments was impossible. As described earlier,<sup>34</sup> in the microsecond transient absorption spectrum of 9DPhen in solvents of different polarity, a clear shift of the absorption bands was observed. Based on this solvent dependence and the observation of a different phosphorescence for 9DPhen and 9-ethylphenanthrene, a more polar triplet state was assumed as in the case of 3,5Me9DPhen.

It has been shown that in systems where the energy is stored in long-living polar excited states (polar triplet states), two different contributions can be distinguished from the volume changes observed in the optoacoustic experiments.<sup>47</sup> The first contribution is the difference in volume between products and reactants and the second contribution contains the contraction or expansion of the medium caused by the release of heat. This is probably the reason why 3,5Me9DPhen (local excited triplet state) yielded good results in the optoacoustic experiments compared to 9DPhen (delocalized excited triplet state).



## Conclusions

From the comparison of the steady-state absorption spectrum of 9DPhen and 3,5Me9DPhen, one can distinguish the different nature of the ground state in both compounds. In 9DPhen the solvent dependence of the CT absorption maximum represents an essential coupling between the two subunits in the ground state compared to 3,5Me9DPhen where the two moieties are decoupled. The bathochromic shift of the emission spectrum of both compounds gives an indication of a substantial dipole moment in the excited state.

The lower values of the radiative rate constant  $\langle k_r \rangle$  and the longer decay times of 3,5Me9DPhen correlate with a less allowed radiative transition compared to that of 9DPhen. It is suggested that for 3,5Me9DPhen, the emissive state mixes to a smaller extent with a state with a strongly allowed transition and/or that the average angle between the phenyl and phenanthrene moieties of the excited state is larger (farther away from 0) than in the unsubstituted molecule, leading to a less allowed transition and a smaller value of the rate constant of fluorescence.

The difference in the microsecond transient absorption spectrum of 9DPhen and 3,5Me9DPhen is an indication of the important difference in the nature of the triplet states in both compounds, which is also found in the optoacoustic experiments.

From the results of the femtosecond transient absorption experiments, a possible model is proposed to characterize the kinetics of these molecules. After photoexcitation of 9DPhen and 3,5Me9DPhen, the distribution of higher excited states shows a fast transition within a femtosecond time scale to a "hot" charge-transfer state. This state loses excess energy by a relaxation process (electronic and/or vibrational and/or conformational relaxation) on a picosecond time scale. From this relaxed excited charge-transfer state, fluorescence and intersystem crossing to a triplet state originate simultaneously and in competition.

The nanosecond transient absorption experiments in combination with the femtosecond transient absorption measurements again show the important difference between the triplet states in 9DPhen and 3,5Me9DPhen.

**Acknowledgment.** A.O. thanks the I.W.T. for financial support. M.V.D.A. is an "Onderzoeksleider" of the Belgian "Fonds voor Kollektief Fundamenteel Onderzoek". The continuing support of the Belgian "Fonds voor Kollektief Fundamenteel Onderzoek" and the DWTC through IUAP-II-16 and IUAP-II-040 is gratefully acknowledged. We thank Professor P. Barbara for his helpful discussions.

## References and Notes

- Rettig, W. *Angew. Chem., Int. Ed. Engl.* **1986**, *25*, 971.
- Hagopian, S.; Singer, L. A. *J. Am. Chem. Soc.* **1985**, *107*, 1874.
- Detzer, N.; Baumann, W.; Schwager, B.; Fröhling, J.-C.; Brittinger, C. *Z. Naturforsch.* **1987**, *A42*, 395.
- Siemiarczuk, A.; Koput, J.; Pohorillo, A. *Z. Naturforsch.* **1982**, *A37*, 598.
- Herbich, J.; Kapturkiewicz, A. *Chem. Phys.* **1991**, *158*, 143, and references therein.
- Herbich, J.; Kapturkiewicz, A. *Chem. Phys.* **1993**, *170*, 221.
- Okada, T.; Fujita, T.; Kubota, M.; Masaki, S.; Mataga, N.; Ide, R.; Sakata, Y.; Misumi, S. *Chem. Phys. Lett.* **1972**, *14*, 563.
- Okada, T.; Fujita, T.; Mataga, N. *Z. Phys. Chem.* **1976**, *101*, 57.
- Masaki, S.; Okada, T.; Mataga, N.; Sakata, Y.; Misumi, S. *Bull. Chem. Soc. Jpn.* **1976**, *49*, 1277.
- Chandross, E. A.; Gordon, M.; Ware, W. R., Eds. *The Exciplex*; Academic Press: New York, 1975; p 187.
- Grabowski, Z. R.; Rotkiewicz, K.; Siemiarczuk, A.; Cowley, D. J.; Baumann, W. *Nouv. J. Chim.* **1979**, *3*, 443.
- Grabowski, Z. R.; Dobkowski, J. *Pure Appl. Chem.* **1983**, *55*, 245.
- Grabowski, Z. R. *Acta Phys. Pol.* **1987**, *A71*, 743.
- Grabowski, Z. R. In *Supramolecular Photochemistry*; Balzani, V., Eds.; Reidel: Dordrecht, 1987; p 319.
- Siemiarczuk, A.; Grabowski, Z. R.; Krówczynski, A.; Asher, M.; Ottolenghi, M. *Chem. Phys. Lett.* **1977**, *51*, 315.
- Grabowski, Z. R.; Rotkiewicz, K.; Siemiarczuk, A. *J. Lumin.* **1979**, *18/19*, 420.
- Siemiarczuk, A. *Chem. Phys. Lett.* **1984**, *110*, 437.
- Siemiarczuk, A.; Ware, W. R. *J. Phys. Chem.* **1987**, *91*, 3677.
- Baumann, W.; Petzke, F.; Loosen, K. D. *Z. Naturforsch.* **1979**, *A34*, 1070.
- Baumann, W.; Bischof, H. *J. Mol. Struct.* **1982**, *84*, 181.
- Detzer, N.; Baumann, W.; Schwager, B.; Fröhling, J. C.; Brittinger, C. *Z. Naturforsch.* **1987**, *A42*, 395.
- Okada, T.; Kawai, M.; Ikemachi, T.; Mataga, N.; Sakata, Y.; Misumi, S.; Shionoya, S. *J. Phys. Chem.* **1984**, *88*, 1976.
- Okada, T.; Mataga, N.; Baumann, W.; Siemiarczuk, A. *J. Phys. Chem.* **1987**, *91*, 4490.
- Baumann, W.; Schwager, B.; Detzer, N.; Okada, T.; Mataga, N. *J. Phys. Chem.* **1988**, *92*, 3742.
- Mataga, N.; Yao, H.; Okada, T.; Rettig, W. *J. Phys. Chem.* **1989**, *93*, 3383.
- Mataga, N.; Nishikawa, S.; Asahi, T.; Okada, T. *J. Phys. Chem.* **1990**, *94*, 1443.
- Barbara, P. F.; Jarzaba, W. In *Advances in Photochemistry*; Volman, D. H., Hammond, G. S., Gollnick, C., Eds.; Wiley: New York, 1990; Vol. 15, p 1.
- Tseng, J. C. C.; Huang, S.; Singer, L. A. *Chem. Phys. Lett.* **1988**, *153*, 401.
- Tseng, J. C. C.; Singer, L. A. *J. Phys. Chem.* **1989**, *93*, 7092.
- Rettig, W.; Baumann, W. In *Photochemistry and Photophysics*; Rabek, J. F., Ed.; CRC Press: Boca Raton, FL, 1992; Vol. 6, p 79.
- Rettig, W. *Top. Curr. Chem.* **1994**, *169*, 253.
- Okada, T. *Proc. Indian Acad. Sci., Chem. Sci.* **1992**, *104*, 173.
- Klock, A. M.; Rettig, W. *Pol. J. Chem.* **1993**, *67*, 1375.
- Onkelinx, A.; De Schryver, F. C.; Viaene, L.; Van der Auweraer, M.; Iwai, K.; Yamamoto, M.; Ichikawa, M.; Masuhara, H.; Maus, M.; Rettig, W. *J. Am. Chem. Soc.* **1996**, *118* (12), 2892.
- Mumada, M. *Pure Appl. Chem.* **1980**, *52*, 669.
- Tomaschewski, G. *J. Prakt. Chem.* **1966**, *33*, 168.
- Morris, J. V.; Mahaney, M. A.; Huber, J. R. *J. Phys. Chem.* **1976**, *80*, 969.
- Khalil, M. M. H.; Boens, N.; Van der Auweraer, M.; Ameloot, M.; Andriessen, R.; Hofkens, J.; De Schryver, F. C. *J. Phys. Chem.* **1991**, *95*, 9375.
- Boens, N.; Janssens, L. D.; De Schryver, F. C. *Biophys. Chem.* **1989**, *33*, 77.
- Boens, N. *Luminiscence Techniques in Chemical and Biochemical Analysis*; De Keukeleire, D., Korkidis, K., Eds.; Marcel Dekker: New York, 1991; p 21.
- Viaene, L.; Van Mingroot, H.; Van haver, P.; Van der Auweraer, M.; De Schryver, F. C.; Itaya, A.; Masuhara, H. *J. Photochem. Photobiol. A* **1992**, *66*, 1.
- Asahi, T.; Matsuo, M.; Masuhara, H. *Chem. Phys. Lett.* **1996**, *256*, 525. Asahi, T.; Matsuo, M.; Masuhara, H.; Koshima, K. *J. Phys. Chem.*, in press.
- Land, E. J. *Proc. R. Soc. London, Ser. A* **1968**, *305*, 457. Windsor, M. W.; Novak, J. R. In *The Triplet State*; Zahlan, A. B., Ed.; Cambridge University Press: London, 1967; p 288.
- Shida, T.; Iwata, S. *J. Am. Chem. Soc.* **1973**, *95*, 3473.
- Herbich, J.; Dobkowski, J.; Rullière, C.; Nowacki, J. *J. Lumin.* **1989**, *44*, 87; **1990**, *46*, 67 (erratum).
- Vandommelen, L.; Boens, N.; Ameloot, M.; De Schryver, F. C.; Kowalczyk, A. *J. Phys. Chem.* **1993**, *97* (45), 11738.
- Callis, J. B.; Parson, W. W.; Gouterman, M. *Biochim. Biophys. Acta* **1972**, *267*, 348. Arata, H.; Parson, W. W. *Biochim. Biophys. Acta* **1981**, *363*, 70. Braslavsky, S. E.; Heibel, G. E. *Chem. Rev.* **1992**, *92*, 1381. Jiwan, J. L.; Chibisov, A. K.; Braslavsky, S. E. *J. Phys. Chem.* **1995**, *99*, 10246. Malkin, S.; Churio, M. S.; Shochat, S.; Braslavsky, S. E. *J. Photochem. Photobiol. B* **1994**, *23*, 79. Jiwan, J. L. H.; Wegewijs, B.; Indelli, M. T.; Scandola, F.; Braslavsky, S. E. *Recl. Trav. Chim. Pays-Bas* **1995**, *114*, 11.